Article

Current Biology

Spatial Working Memory in Humans Depends on Theta and High Gamma Synchronization in the Prefrontal Cortex

Graphical Abstract

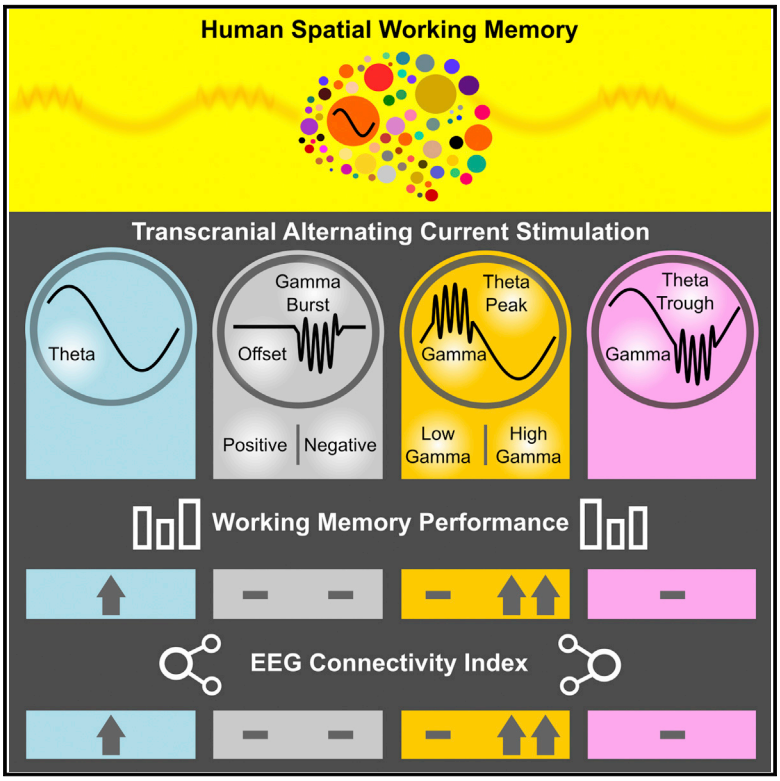

Highlights

- Both theta and theta-gamma tACS improve working memory performance
- Theta-gamma tACS protocols have greater effect on working memory than theta tACS
- High gamma power over the peak, but not over the trough, of theta wave boosts memory
- The optimal gamma frequencies manifest in the 80 to 100 Hz frequency range

Authors

Ivan Alekseichuk, Zsolt Turi, Gabriel Amador de Lara, Andrea Antal, Walter Paulus

Correspondence

ivan.alekseichuk@med.uni-goettingen.de

In Brief

Alekseichuk et al. demonstrate the role of theta-gamma cross-frequency coupling in human prefrontal cortex for working memory by using causal inference. They applied cross-frequency transcranial alternating current stimulation and showed the phase and frequency specificity of theta-gamma rhythms during working memory performance.

Alekseichuk et al., 2016, Current Biology *26*, 1513–1521
June 20, 2016
http://dx.doi.org/10.1016/j.cub.2016.04.035

Current Biology
Article

Spatial Working Memory in Humans Depends on Theta and High Gamma Synchronization in the Prefrontal Cortex

Ivan Alekseichuk,[1,*] Zsolt Turi,[1] Gabriel Amador de Lara,[1] Andrea Antal,[1] and Walter Paulus[1]
[1]Department of Clinical Neurophysiology, University Medical Centre Göttingen, Georg-August University Göttingen, 37075 Göttingen, Germany
*Correspondence: ivan.alekseichuk@med.uni-goettingen.de
http://dx.doi.org/10.1016/j.cub.2016.04.035

SUMMARY

Previous, albeit correlative, findings have shown that the neural mechanisms underlying working memory critically require cross-structural and cross-frequency coupling mechanisms between theta and gamma neural oscillations. However, the direct causality between cross-frequency coupling and working memory performance remains to be demonstrated. Here we externally modulated the interaction of theta and gamma rhythms in the prefrontal cortex using novel cross-frequency protocols of transcranial alternating current stimulation to affect spatial working memory performance in humans. Enhancement of working memory performance and increase of global neocortical connectivity were observed when bursts of high gamma oscillations (80–100 Hz) coincided with the peaks of the theta waves, whereas superimposition on the trough of the theta wave and low gamma frequency protocols were ineffective. Thus, our results demonstrate the sensitivity of working memory performance and global neocortical connectivity to the phase and rhythm of the externally driven theta-gamma cross-frequency synchronization.

INTRODUCTION

The past decade has seen advances in neuronal recording and analytical techniques that extend our understanding of brain waves as manifestations of a complex system characterized by both single rhythms and critical cross-frequency features [1, 2]. The multilevel organization of brain oscillations integrates functional brain systems across multiple spatiotemporal scales [3, 4], and thus implies a sophisticated solution for the highly precise temporal coordination between the fast local neuronal computations with external input and the global system state [5, 6]. In order to effectively propagate and maintain information in neural networks, neurons form assembly sequences that give rise to mesoscopic and macroscopic network oscillations. These are characterized by cross-frequency phase-amplitude coupling [7]—the phenomenon of synchronization between the power and the phase of fast and slow oscillations [1]. Cross-frequency coupling has been detected both in the hippocampal and neocortical areas and is associated with multiple cognitive processes, including memory and attention [8, 9]. We may hypothesize that the complex organization of neuronal activity is especially important for computationally demanding cognitive processes, such as working memory. Working memory refers to the ability to maintain short-term information, and forms the basis of numerous cognitive processes. The multiplexing buffer model of working memory holds that short-term information is represented by the ordered activity of cell assemblies and that the multiple items retained in working memory are organized by theta-nested gamma subcycles [5]. A key assumption of this model is that the different gamma subcycles representing local neural computations correspond to different theta phases, which allows information maintenance and separation via oscillatory activity [5]. Here, in order to demonstrate the essential role of cross-frequency coupling in spatial working memory, neuronal oscillations in one of the key anatomical areas, i.e., the left prefrontal cortex [10, 11], were entrained by transcranial alternating current stimulation (tACS) while the study volunteers performed a spatial working memory task. According to the prevailing view, tACS entrainment leads to a frequency-specific phase realignment of the endogenous oscillations with the applied alternating current, as well as to a frequency-specific power enhancement [12–15]. In this study, conventional continuous theta (6 Hz) stimulation was applied as a standard effective intervention in the working memory function [16, 17]. Furthermore, considering the correlation between increased theta-gamma coupling and successful item memorization in the working memory tasks [18, 19], we introduced continuous theta and repetitive gamma co-stimulation—cross-frequency tACS (Figure 2)—with the aim of mimicking the natural distribution of gamma power over the theta cycle in the neocortex. We hypothesized that magnification of high gamma oscillations during the peaks or troughs of the theta wave would strengthen or weaken the endogenous coupling, and thus facilitate or hinder the informational processing in the affected brain area. Accordingly, it should also affect the corresponding functional network, leading to a detectable impact on performance. This would not only confirm an organizing role of phase-amplitude coupling but also pave the way for developing more elaborate stimulation paradigms for entrainment of ongoing brain activity.

In the present work, we demonstrate the true causal role of phase-amplitude coupling in healthy humans by linking

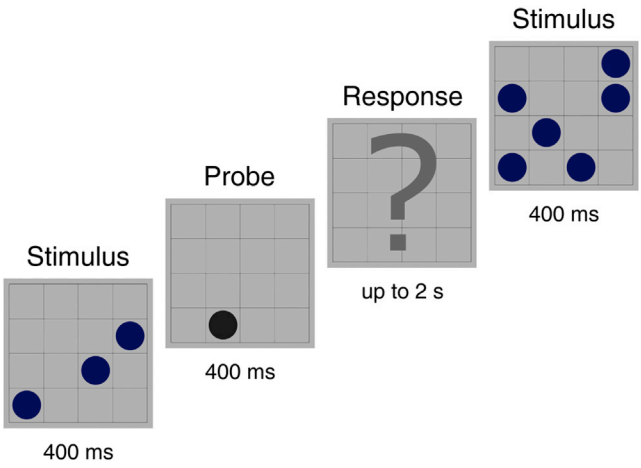

Figure 1. Working Memory Test

During each session, participants performed a two-back visual-spatial match-to-sample test, which is commonly used to assess spatial working memory performance [30]. The test consisted of 80 trials. In each trial, there were three events separated by 1 to 2 s intervals: a stimulus (appearance of three or six dots on the screen), a test image (appearance of a single dot on the screen), and a response period. Volunteers were asked to press the "yes" or "no" button during the response period indicating whether the location of the dot in the test image matched the stimulus in the previous trial (two-back condition).

behavioral performance in a spatial working memory test and modulation of electroencephalogram (EEG) connectivity with the features of tACS entrainment. The present findings show that co-stimulation of theta and gamma waves in the prefrontal cortex boosts spatial working memory only when repetitive gamma bursts are phase locked to the peaks of theta rhythm. Furthermore, we also show that the optimal high gamma frequencies for multi-item retention were between 80 and 100 Hz in the prefrontal cortex.

RESULTS

During the experimental sessions, our volunteers performed one of the predefined versions of the visual-spatial working memory task (Figure 1). The order of the sessions and the versions of the task were randomized and counterbalanced across the volunteers. The individual hit rates and false alarm rates were collected to determine the behavioral outcomes of the intervention. According to signal detection theory [20], memory effectiveness in a given condition is estimated as follows: sensitivity index $d' = Z(\text{"hit rate"}) - Z(\text{"false alarm rate"})$, where $Z(p)$, $p \in [0,1]$. The tACS was applied over the left prefrontal cortex simultaneously with the administration of the memory test (Figure 2C). Resting-state EEGs were recorded immediately before and after the test and stimulation procedures, and were further analyzed to estimate the phase connectivity.

Theta-Gamma Coupling Organizes Spatial Working Memory

In the first set of experiments, we evaluated the spatial working memory performance of the volunteers while they were receiving sham stimulation (*Control*), continuous single-frequency theta stimulation (*SF-6*), or cross-frequency tACS between the theta and gamma frequencies (Figures 2A and 2B, *CF-6,80p* and *CF-6,80t*). The subject-specific effect of the stimulation on d′ was then modeled using the generalized linear mixed-effect approach. The subsequent marginal ANOVA test demonstrated the significance of the stimulation on memory performance ($F_{3,60} = 5.04$, $p = 0.004$). The following pairwise bootstrap t test (5,000 iterations, $p \leq 0.05$) revealed that whereas continuous theta stimulation improved memory performance as expected (Figure 3A), the effect of the cross-frequency stimulation depended on the resulting phase-amplitude structure of the stimulation signal. Synchronization of high gamma bursts with the troughs of theta oscillation cancelled out the positive effect of the continuous low-frequency entrainment per se; however, the opposite pattern strongly increased its effectiveness. Effect size in terms of standardized mean difference was estimated for each condition relative to the sham stimulation: $g_{SF\text{-}6} = 0.19$, $g_{CF\text{-}6,80t} = 0.1$, and $g_{CF\text{-}6,80p} = 0.48$.

Analysis of the reaction time revealed no significant changes with respect to the stimulation (Figure 3D; $F_{3,60} = 0.72$, $p = 0.54$). The effect of the session order on memory performance was insignificant according to the linear regression model ($p = 0.76$, $R^2 = 0.02$).

In the next step, we evaluated how modification of memory performance was reflected by changes in brain activity. This revealed a strong association between the increase in global phase connectivity and improvement of spatial working memory. The connectivity index (CI), which expresses the proportion of sensor pairs that demonstrate a significant increase in the weighted phase lag index, showed a clear-cut difference between the conditions (Figures 5A and 5D): the changes in phase connectivity were minor after placebo and ineffective stimulations ($CI_{Control} = 0.024$ and $CI_{CF\text{-}6,80t} = 0.005$) but significant after the successful intervention in the working memory process ($CI_{SF\text{-}6} = 0.090$ and $CI_{CF\text{-}6,80p} = 0.105$). The permutation test indicated that $CI = 0.075$ corresponded to the significance level 5%.

Looking at the behavioral and electrophysiological data together, we can conclude that cross-frequency tACS effectively enhances working memory performance in the affected brain area, but only if the high gamma oscillations are synchronized with the theta wave peaks. These results suggest that maintenance of the exact temporal organization of high gamma power fluctuations and theta phase is not only a correlative phenomenon but also an important prerequisite for the successful storage, manipulation, and/or recall of information in spatial working memory.

Frequency Specificity of High Gamma Oscillations

Based on the results of the first experiment, one of the most interesting questions was the importance of the exact frequency of the fast oscillatory activity for the maintenance of theta-gamma coupling. Although the characteristics of theta rhythm in the neocortex and its role in memory processes are relatively well known [19, 21], there are contradictory data regarding the frequency band and the optimum memory-related point of high gamma rhythm. Some of the previous correlative findings suggest that spatial working memory performance may be explained by theta phase-locked power fluctuations in the range of 60–100 Hz [11, 22], whereas other datasets demonstrate the greater involvement of faster oscillations (100–200 Hz) [23–26].

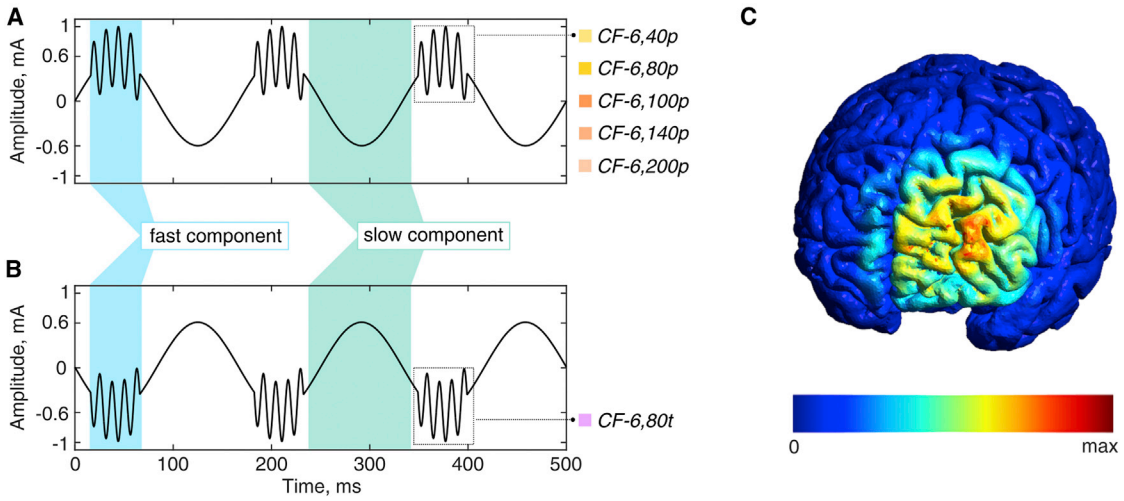

Figure 2. Main Stimulation Parameters

(A and B) Principal waveforms of the cross-frequency transcranial alternating current stimulation (tACS) protocols: repetitive bursts of fast alternating current superimposed on the peaks (A) or troughs (B) of the continuous, slow alternating current. The frequency of the continuous component was 6 Hz for all experimental conditions, which is thought to correspond to the theta range in the human neocortex. Fast bursts were applied with a frequency of 40 Hz (*CF-6,40p*), 80 Hz (*CF-6,80p* and *CF-6,80t*), 100 Hz (*CF-6,100p*), 140 Hz (*CF-6,140p*), or 200 Hz (*CF-6,200p*), covering the gamma range. Cross-frequency tACS was delivered at a peak-to-baseline intensity of 1 mA, where 0.6 mA was dedicated to the low-frequency component.

(C) Simulation of the applied electric field. The realistic, finite element head model included five compartments: scalp, bone, cerebrospinal fluid, gray matter, and white matter. The maximum strength of the electric field is color coded from 0 to 0.35 mV/mm.

Moreover, there is a little doubt that these parameters highly depend on the anatomical structures and the types of cognitive tasks. Thus, for the second experiment, we modified the most successful stimulation protocol for cross-frequency tACS (*CF-6,80p*) by introducing a new variable—the frequency of the fast oscillatory component (100, 140, and 200 Hz).

The generalized linear mixed-effect model with a subsequent marginal ANOVA test confirmed the stimulation-related improvement in working memory performance (Figure 3B; $F_{3,52} = 2.95$, $p = 0.04$). The complementary bootstrap t test (5,000 iterations, $p \leq 0.05$) showed that spatial working memory performance was significantly strengthened by the tACS at any frequency of the fast oscillatory component in the range of 80–200 Hz, given the gamma bursts synchronization with the theta wave peaks. However, the highest effect size corresponded to the bursts of 80–100 Hz (Figure 4; $g_{CF\text{-}6,80p} = 0.48$ and $g_{CF\text{-}6,100p} = 0.45$), followed by a gradual decrease ($g_{CF\text{-}6,140p} = 0.35$ and $g_{CF\text{-}6,200p} = 0.26$).

No changes in reaction time were observed between the conditions (Figure 3E; $F_{3,52} = 0.34$, $p = 0.79$). The effect of the session order on memory performance was tested using linear regression ($p = 0.92$, $R^2 = 0.01$).

We also considered the impact of cross-frequency electrical interventions on the brain state. These results confirm the association between the prominent increase in phase connectivity and successful tACS intervention (Figures 5B and 5E). The connectivity index, as the measurement of the global changes in the phase lag index, reached the levels $CI_{CF\text{-}6,100p} = 0.119$, $CI_{CF\text{-}6,140p} = 0.100$, and $CI_{CF\text{-}6,200p} = 0.091$, compared to the insignificant increase after sham stimulation ($CI_{Control} = 0.043$). The permutation test indicated that CI = 0.075 corresponded to the significance level 5%.

The results of the second experiment suggest that cross-frequency coupling is characterized by the relatively stable parameters, not only in the time domain but also with regard to frequency. It seems reasonable to speculate that the optimal timing and rhythm are tightly linked to the properties of the functional as well as anatomical substrate. Here we were able to demonstrate the feasibility of experimental rectification of phase-amplitude coupling in the neocortex; further experiments might narrow the optimal parameters even more. Furthermore, our data suggest that theta-gamma coupling is manifested within a range of effective frequencies, rather than embodied in a single exact oscillation. This observation is consistent with the idea that functional brain networks have an optimal physiological state, with a range of sub-optimal configurations that eventually fall into a different, non-optimal state for a given task.

Control Experiment

To confirm the essential role of the interaction between slow and fast oscillatory components for cross-frequency tACS, we performed the third, control experiment. Bursts of 80 Hz alternating current with positive (*Bursts+*) or negative (*Bursts−*) direct current offset were delivered while the volunteers performed the working memory test. These stimulation conditions could be seen as a variation of the previous protocols *CF-6,80p* and *CF-6,80t* that lacked the continuous 6 Hz component. In addition, cross-frequency tACS with low-frequency gamma rhythm (40 Hz) as the faster component—condition *CF-6,40p*—was introduced to clarify the frequency specificity of the observed effects with regard to gamma rhythm involvement. Here, the generalized linear mixed-effect model showed no significant effects of the stimulations on working memory performance (Figure 3C; $F_{3,56} = 0.51$, $p = 0.68$). Evaluation of the global EEG phase

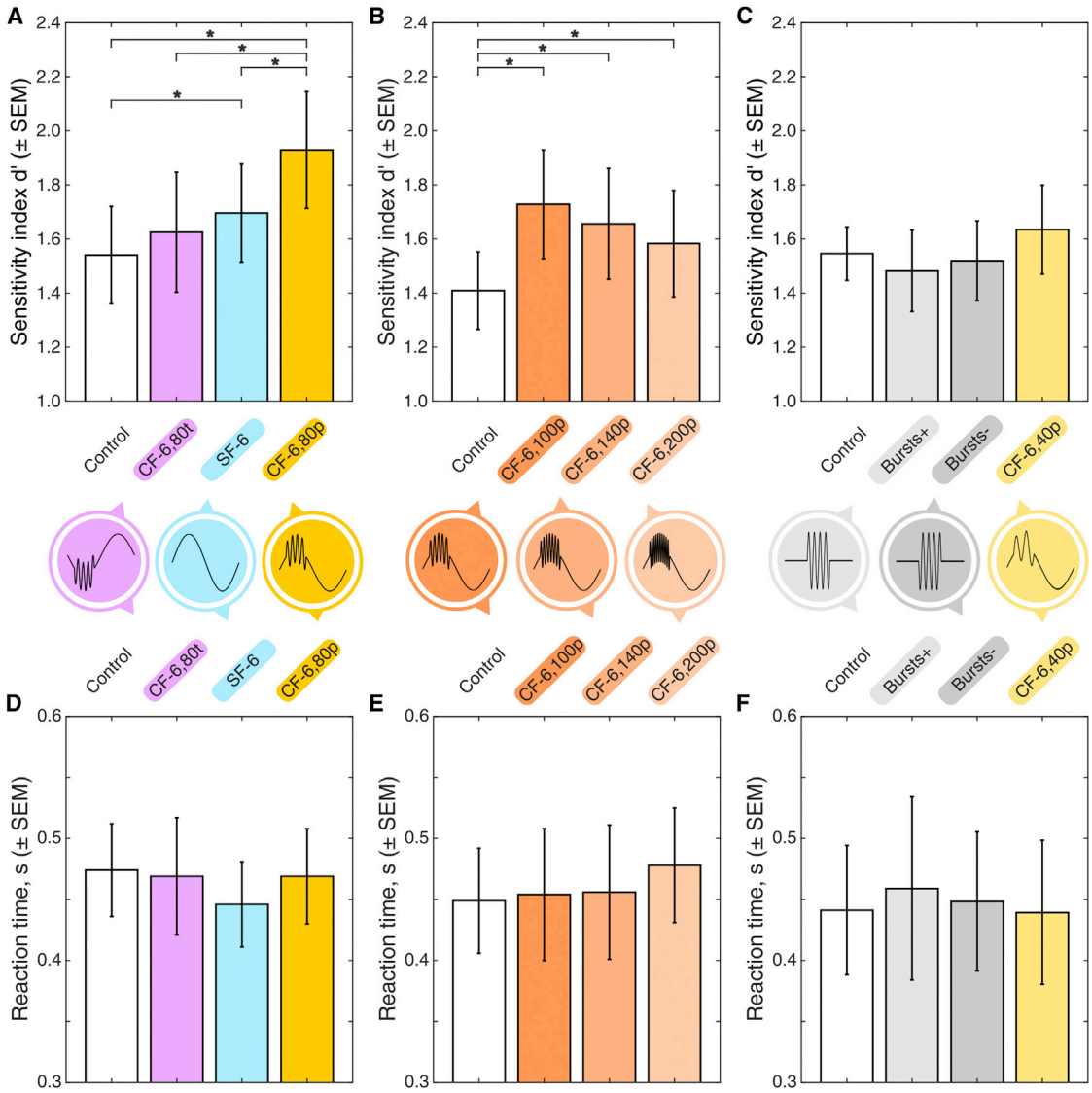

Figure 3. Working Memory Performance

(A–C) Mean working memory performance in terms of sensitivity index d′ was estimated for the following conditions: (A) sham stimulation (*Control*); continuous 6 Hz tACS (*SF-6*); (B) cross-frequency tACS between 6 Hz and 40, 80, 100, 140, and 200 Hz (*CF-6,40p*, *CF-6,80t*, *CF-6,80p*, *CF-6,100p*, *CF-6,140p*, and *CF-6,200p*); and (C) bursts of 80 Hz tACS with positive or negative direct current offset (*Bursts+* and *Bursts−*). Horizontal brackets show statistically significant paired differences according to the bootstrap t test (*$p \leq 0.05$). Colored clouds below the figure depict the corresponding stimulation waveforms.

(D–F) Mean reaction time during the memory test. No statistically significant differences were observed according to the generalized linear mixed-effect model ($p \leq 0.05$).

connectivity before and after the test confirmed no impact of the given stimulation conditions (Figures 5C and 5F). In comparison to the previous data, these results refute two alternative possibilities: (1) that high gamma bursts alone can be responsible for the improvement in working memory during cross-frequency tACS, and (2) that low-frequency gamma rhythm in the prefrontal cortex reflects the same processes as high-frequency gamma oscillations. This is apparent, because for the given visual-spatial working memory test, entrainment of 40 Hz activity in the prefrontal cortex did not improve performance. Moreover, no changes in the reaction time (Figure 3F; $F_{3,56} = 0.53$, $p = 0.66$) were observed. Taken together, these findings further support the crucial role of the theta and high gamma interplay in the prefrontal cortex during working memory tasks.

DISCUSSION

The aim of the current study was to investigate the causal role of theta-gamma phase-amplitude coupling during spatial working memory in humans. To entrain neural oscillatory activity in a non-invasive and reversible manner, we used tACS selectively over the left prefrontal cortex, which is a key node in a network that underpins human spatial working memory [10, 11, 27]. In order to investigate the potential effects of biologically relevant

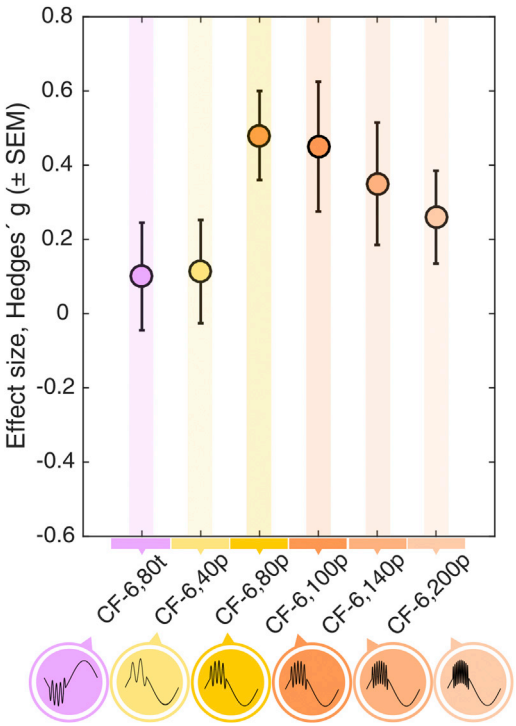

Figure 4. Improvement of the Performance during Cross-Frequency tACS

Effect sizes of the cross-frequency tACS protocols *CF-6,80t* (80 Hz bursts over the troughs of 6 Hz waves), *CF-6,40p*, *CF-6,80p*, *CF-6,100p*, *CF-6,140p*, and *CF-6,200p* (40, 80, 100, 140, and 200 Hz bursts over the peaks of 6 Hz waves, as illustrated by colored clouds) on working memory performance relative to sham stimulation in terms of standardized mean difference. Calculations were done using the debiased estimator Hedges' g.

oscillatory activities and their exact spatiotemporal relations, we used traditional, single-frequency as well as novel, cross-frequency tACS protocols. These aimed to mimic the gamma power distribution over the theta cycles that are natural characteristics of the neural oscillatory pattern during working memory performance [5]. Our behavioral and electrophysiological analyses revealed three main findings: (1) both single-frequency and cross-frequency tACS altered the EEG characteristics of the brain state and boosted spatial working memory performance; (2) cross-frequency tACS was superior to single-frequency tACS when the gamma-burst stimulation was superimposed on the theta peak; and (3) the optimal frequency of the fast oscillatory component in cross-frequency tACS was not restricted to a single exact frequency but rather characterized by a relatively wide frequency range between 80 and 100 Hz.

Solving a spatial working memory task requires the retention of spatial information in the absence of the external stimulus, which anatomically involves a distributed network that includes the prefrontal and posterior-parietal cortex as well as the basal-ganglia and hippocampal formation [28, 29]. Effective information transmission across neural structures requires the spatiotemporal coordination of oscillatory activity, which was recently crystallized into the theory of oscillatory hierarchy [30, 31]. A growing body of correlative results suggests that slower frequencies, such as theta oscillation, that are capable of integrating a larger number of neurons, promote this cross-structural, cross-frequency neural communication [26, 32]. It was proposed that theta rhythm forms a temporal structure that organizes gamma-encoded units (like "shelves in a closet"), thus preventing them from mixing, and allows for careful processing and transmission of neural computations [33]. However, there is a longstanding debate about whether the voltage fluctuation in the extracellular medium generated by the synchronous population activity has any functional relevance or whether it is a mere epiphenomenon [34]. According to the ephaptic coupling hypothesis [35], the extracellular voltage gradient indeed plays a functional feedback role—e.g., by influencing spike field coherence—and affects membrane potential. To reveal the true functional role of the cross-frequency characteristics of the extracellular field, we artificially manipulated the electrical landscape of the prefrontal cortex by means of novel tACS protocols. In the present work, we provided sufficient evidence for the functional importance of the extracellular voltage gradient by generating a low-amplitude synthetic electric field that mimics theta-gamma phase-amplitude coupling in spatial working memory under physiological conditions. Earlier studies have shown that low-intensity external fields (as weak as 0.2–0.3 mV/mm) can exert detectable influence on physiologically occurring local neural activity, despite its higher magnitude (approximately 2–4 mV/mm) [36, 37].

According to the reader-initiated neural communication concept, neural information transfer between the "sender" and the "reader" networks is controlled by the network dynamics, mainly phase, of the reader network. Indeed, one key assumption of the multiplexing buffer working memory model is that gamma subcycles are nested in preferred phases of the theta cycle. Our findings are in compelling agreement with the predictions of these models, as cross-frequency tACS protocols were only effective when gamma bursts were superimposed on the peak, and not on the trough, of the theta cycle. Moreover, we demonstrated a potential application of the cross-frequency concept for non-invasively altering the brain state and boosting working memory performance. Our results also have clinical relevance; numerous studies have reported abnormal cross-frequency coupling during the course of certain neurological and mental disorders, such as Parkinson's syndrome, schizophrenia, and anxiety [38, 39].

However, detailed investigation is needed to clarify specifically the behavioral relevance of cross-frequency tACS, and whether its effect operates at the encoding, maintenance, or recollection stages. Also, further research is needed to reveal whether cross-frequency tACS in the prefrontal cortex directly modulates high gamma oscillations. Because the present study utilized surface EEG to characterize the brain state prior to and following tACS, the investigation of high gamma oscillation was technically not feasible. Advancing our knowledge of the effect of cross-frequency tACS on oscillatory activity will require the use of additional neuroimaging techniques, such as electrocorticography or magnetoencephalography.

Overall, the present results support and extend the theory of cross-frequency organization of the oscillations in the neocortex. We demonstrated the dependence of spatial working memory function on the phase-amplitude organization of the entrained

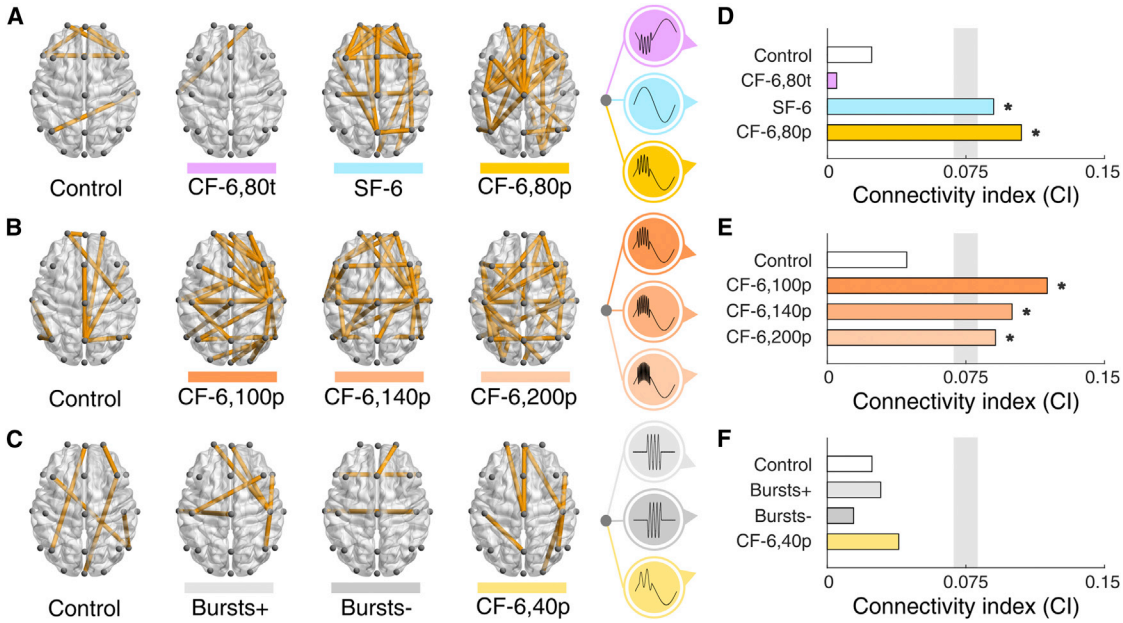

Figure 5. Phase Connectivity Difference Maps

(A–C) Resting-state EEG was recorded during every session for 3 min immediately before and after the test-stimulation procedure. In order to quantify the changes in brain state, phase connectivity was estimated using the debiased weighted phase lag index algorithm and compared with the non-parametric bootstrap t test ($p \leq 0.01$). In the figure, pairs of sensors that exhibited a significant post-test increase of phase connectivity are linked. Stimulation waveforms are illustrated by colored clouds.

(D–F) Connectivity index represents the global increase in phase connectivity for a given condition. The gray zone denotes the level of statistical significance according to the permutation test (*$p \leq 0.05$). Please see Figure S1 regarding the correlations between the phase connectivity and working memory performance.

theta and gamma rhythms as well as the reasonable frequency specificity of this entrainment. Further investigations into cross-frequency coupling to clarify the role of multiple stimulation sites and the intensity relation between theta and gamma activity promise an interesting avenue of scientific research and clinical practice.

EXPERIMENTAL PROCEDURES

Participants

Forty-seven healthy, adult volunteers (25 females, ages 19–28) with normal or corrected-to-normal vision were recruited for the study after having given written informed consent. None of the participants had symptoms or history of neurological or psychiatric disorders, brain injury, or drug-dependent chronic conditions. Twelve volunteers reported previous experience with transcranial electrical stimulation. All participants were naive with respect to the cognitive test.

Sixteen volunteers completed the first experiment, and 14 completed the second. In the second experiment, 2 volunteers did not appear for all sessions, and their data were excluded from analysis. An additional 15 volunteers were enrolled in the control experiment. None of the participants reported any stimulation-related side effects during or after the sessions.

All experiments were conducted in accordance with the Declaration of Helsinki and with the approval of the ethics committee of the Georg-August University Göttingen.

Experimental Procedure

Three experiments were conducted successively with separate recruitment calls. Each experiment included four sessions in a randomized and counterbalanced order. Sessions were separated by at least 48 hr. All volunteers attended a personal introductory meeting where they were familiarized with the laboratory and the procedure. Every session consisted of (1) a pre-stimulation, resting-state EEG recording, (2) a working memory test, and (3) a post-stimulation, resting-state EEG recording. tACS was applied while the participants performed the working memory task.

Working Memory Test

Participants performed the two-back version of the visual-spatial match-to-sample test [11]. The test was generated with PsychoPy software [40]. It consisted of 80 trials and required approximately 9 min to complete (Figure 1). In each trial, there were three events separated by intervals of 1–2 s: a stimulus (the appearance of a group of three or six dark blue dots on the screen), a test image (the appearance of a single black dot on the screen), and a response period. Volunteers were requested to press the "yes" or "no" button during the response period, indicating whether the location of the dot in the test image matched the stimulus in the two-back trial. The order of trials was pseudo-randomized across the sessions. Responses were acquired using a dedicated response pad (RB-740; Cedrus).

EEG and Transcranial Alternating Current Stimulation

All experiments were conducted in a laboratory shielded from sound and electromagnetic signals. Electrical stimulation and recording were carried out using the specialized EEG-tACS system NEXT WAVE (EBS Technologies). The EEG was recorded against a common average reference signal using the passive Ag/AgCl electrodes applied to 21 standard positions according to the international 10-20 system. The sampling rate was 2 kHz at an analog-digital precision of 24 bits.

Stimulation was delivered via five flat, round, rubber electrodes (r 1 cm), which were affixed with conductive paste under the EEG cap. The central electrode was positioned over the AF3 position according to the international 10-10 system, and four opposing electrodes were equally spaced at a distance of 6 cm from AF3 (Figure 2C). The sampling rate of the stimulation signal was 1 MHz at an analog-digital precision of 14 bits ($\approx 0.5\ \mu A$). A 1 mA peak-to-baseline alternating current was applied for 10 min during the memory test procedure, which included 10 s fade-in and fade-out periods. Impedance was kept below 10 kOhm.

Sham Stimulation: Control

In the first and third experiments, electrical current was applied for short periods (30 s) at the beginning of the session and then turned off. This procedure induces skin sensations similar to the real stimulation without any detectable impact on the brain state [41]. In the second experiment, in order to control for possible saturation of the recording electrodes, tACS was applied with a frequency of 80 Hz for the entire time, but at a lower intensity (0.2 mA peak to baseline). This low-intensity stimulation has no known effect on cortical excitability, and should not have had a significant effect on any other parameters [42]. Analysis of the performance data revealed no difference between the control conditions.

Single-Frequency Alternating Current Stimulation: SF-6

A continuous, sinusoidal 6 Hz stimulation was applied at an intensity of 1 mA peak to baseline.

Cross-Frequency Alternating Current Stimulation: CF-"Theta-Gamma Frequencies"

This stimulation consisted of two superimposed components: continuous slow wave, and repetitive bursts of fast oscillations. The slow component was the 6 Hz sinusoidal stimulation with 0.6-mA peak-to-baseline current for every corresponding condition. The fast component frequency was 40 Hz (condition *CF-6,40t*), 80 Hz (*CF-6,80t* and *CF-6,80p*), 100 Hz (*CF-6,100p*), 140 Hz (*CF-6,140p*), or 200 Hz (*CF-6,200p*) at 0.4 mA peak to baseline. Bursts were synchronized with the continuous wave and lasted for 50 ms during every trough (*CF-6,80t*) or peak (*CF-6,40p*, *CF-6,80p*, *CF-6,100p*, *CF-6,140p*, and *CF-6,200p*). Temporally accurate fusing of the components was achieved by dedicated hardware and monitored with an oscilloscope.

Gamma-Burst Stimulation: Bursts

Bursts of 80 Hz alternating current were applied for 50 ms six times per s with a current of 0.4 mA peak to baseline with positive or negative DC offset (*Bursts+* or *Bursts−*). Total intensity was equal to 1 mA peak to baseline. These stimulation conditions were designed to reproduce the conditions *CF-6,80t* and *CF-6,80p* without the continuous slow-wave component.

Stimulation Montage

The main stimulation electrode was always positioned over the point AF3 according to the international 10-10 EEG system. Four return electrodes were equally spaced at a distance of 6 cm around the main electrode. This electrode montage was used to affect the left prefrontal cortex. The anatomical target was validated by simulating the applied electric field. The realistic, finite element model was generated and solved using SimNIBS 2 [43, 44]. The following compartments were used in the model: scalp (σ = 0.465 S/m), bone (σ = 0.010 S/m), cerebrospinal fluid (σ = 1.654 S/m), gray matter (σ = 0.275 S/m), and white matter (σ = 0.126 S/m). Post-processing and visualization of the mesh was done using Gmsh [45]. The resulting electric field confirmed the left prefrontal cortex as the target region (Figure 2C).

Working Memory Task

Working memory performance was analyzed using signal detection theory [20]. Hit rates and false alarm rates were combined in the sensitivity index d′ as follows:

$$d' = Z(\text{"hit rate"}) - Z(\text{"false alarm rate"}),$$

where Z(p), $p \in [0,1]$.

According to the theory, sensitivity index d′ represents the distance between the mean of the distribution of signal plus noise from one side and the noise distribution from the other side, where the mean of the noise distribution is zero and both distributions have an SD of one. Applied to cognitive science, d′ is used as the bias-free measure of observer sensitivity in tasks with response. Although the sensitivity index is a dimensionless statistic, we performed the computational simulation of the two-back visual-spatial match-to-sample test to determine the parameters of the random behavior: d′ = 0 ± 0.77 (mean ± 99% confidence interval). Thus, for the given working memory test, the probability that index d′ would exceed 0.77 by chance was less than 0.5%.

In view of the crossover design of our study, the significance of the learning effect was controlled using the linear regression model with "session order" as the categorical predictor variable and d′ as the response variable.

The impact of the stimulation on memory performance was tested using the generalized linear mixed-effect model, where "stimulation condition" was taken as the fixed-effect factor and "participant id" as the random-effect factor. Parameters of the model were estimated using the maximum pseudo-likelihood method and fitted using the log link function. The marginal ANOVA test was applied to estimate the significance of the fixed-effect factor. Subsequently, the non-parametric bootstrap t test ($p \leq 0.05$) was used for pairwise comparisons between the conditions. For this test, the null hypothesis distribution of the T scores was estimated for every comparison using the bootstrapping approach (5,000 iterations). The true observed T score was then compared with the null distribution, and a binary decision was made whether the observed T score had a 5% or less chance to occur under the null hypothesis. Separately, effect size was calculated as the standardized mean difference using the estimator Hedges' g [46] for every real stimulation condition compared to the sham stimulation. In comparison to other approaches, this estimator is debiased with respect to sample size. It is common to interpret Hedges' $g > 0.8$ as a large effect, $g > 0.5$ as a medium effect, and $g > 0.2$ as a small effect.

Connectivity Analysis

EEG data were analyzed using MATLAB 8.5 (MathWorks) with the FieldTrip toolbox [47]. Initially, all datasets were band-pass filtered from 1 to 45 Hz with an eighth-order non-causal Butterworth IIR filter and divided into 2-s-long epochs with 50% overlap. The epochs were then linearly detrended and down-sampled to 1 kHz. They were subsequently semi-automatically analyzed for the presence of ocular and muscular artifacts using the adoptive z threshold. Trials with extreme variance were rejected. Data from 4 sessions out of 180 were excluded entirely, for technical reasons.

Phase connectivity was estimated in the sensor space. First of all, frequency analysis was performed for every trial using the multitaper method. We focused our attention on the frequency band from the half-harmonic (3 Hz) to the second-order harmonic (12 Hz) frequencies around the 6 Hz carrying rhythm that formed the basis of all our tACSs. The debiased weighted phase lag index (wPLI) was computed for every pair of electrodes and averaged across the trials. Compared to other approaches, wPLI has the advantage of low sensitivity to the volume conduction and noise of a different origin [48]. Moreover, it is debiased with respect to sample size.

Finally, for every condition, pre- and post-stimulation phase lag indices were compared by non-parametric bootstrap t tests (5,000 iterations, $p \leq 0.01$) using MATLAB. Phase connectivity difference maps were visualized using BrainNet Viewer [49]. The connectivity index was then estimated for every condition as follows: CI = sp_sig / sp_total, where sp_sig is the number of sensor pairs that demonstrates the significant modulation of connectivity and sp_total is the total number of sensor pairs. A permutation test was introduced to estimate the level of significance. To that end, matrices of the wPLIs corresponding to all conditions before and after the stimulation were randomly permuted to generate dummy data. These data entered the analysis as described above. The procedure was repeated 10,000 times, and the resulting distribution of the connectivity indices was used to estimate the 95% confidence interval. Connectivity indices that exceeded this interval ($CI \geq 0.075$ for the given datasets) were considered statistically significant.

SUPPLEMENTAL INFORMATION

Supplemental Information includes Supplemental Experimental Procedures and one figure and can be found with this article online at http://dx.doi.org/10.1016/j.cub.2016.04.035.

AUTHOR CONTRIBUTIONS

I.A. and W.P. conceptualized the study. I.A., A.A., and W.P. designed the study. I.A., G.A.d.L., and Z.T. collected the data. I.A. analyzed the data. W.P. and A.A. supervised the study. I.A., Z.T., G.A.d.L., A.A., and W.P. wrote the manuscript.

CONFLICTS OF INTEREST

W.P. is on the scientific advisory board of EBS Technologies, which provided the stimulation device. W.P. holds a patent on transcranial deep-brain stimulation.

ACKNOWLEDGMENTS

The authors wish to thank Christine Crozier for proofreading the manuscript. This research was supported by the Deutsche Forschungsgemeinschaft (Priority Program SPP 1665 to W.P.).

Received: October 29, 2015
Revised: April 8, 2016
Accepted: April 13, 2016
Published: May 26, 2016

REFERENCES

1. Canolty, R.T., Edwards, E., Dalal, S.S., Soltani, M., Nagarajan, S.S., Kirsch, H.E., Berger, M.S., Barbaro, N.M., and Knight, R.T. (2006). High gamma power is phase-locked to theta oscillations in human neocortex. Science *313*, 1626–1628.
2. Jensen, O., and Colgin, L.L. (2007). Cross-frequency coupling between neuronal oscillations. Trends Cogn. Sci. *11*, 267–269.
3. Buzsáki, G., Logothetis, N., and Singer, W. (2013). Scaling brain size, keeping timing: evolutionary preservation of brain rhythms. Neuron *80*, 751–764.
4. Staresina, B.P., Bergmann, T.O., Bonnefond, M., van der Meij, R., Jensen, O., Deuker, L., Elger, C.E., Axmacher, N., and Fell, J. (2015). Hierarchical nesting of slow oscillations, spindles and ripples in the human hippocampus during sleep. Nat. Neurosci. *18*, 1679–1686.
5. Lisman, J.E., and Jensen, O. (2013). The theta-gamma neural code. Neuron *77*, 1002–1016.
6. Lisman, J., and Buzsáki, G. (2008). A neural coding scheme formed by the combined function of gamma and theta oscillations. Schizophr. Bull. *34*, 974–980.
7. Buzsáki, G. (2010). Neural syntax: cell assemblies, synapsembles, and readers. Neuron *68*, 362–385.
8. Canolty, R.T., and Knight, R.T. (2010). The functional role of cross-frequency coupling. Trends Cogn. Sci. *14*, 506–515.
9. Axmacher, N., Henseler, M.M., Jensen, O., Weinreich, I., Elger, C.E., and Fell, J. (2010). Cross-frequency coupling supports multi-item working memory in the human hippocampus. Proc. Natl. Acad. Sci. USA *107*, 3228–3233.
10. Barbey, A.K., Colom, R., Paul, E.J., and Grafman, J. (2014). Architecture of fluid intelligence and working memory revealed by lesion mapping. Brain Struct. Funct. *219*, 485–494.
11. Roux, F., Wibral, M., Mohr, H.M., Singer, W., and Uhlhaas, P.J. (2012). Gamma-band activity in human prefrontal cortex codes for the number of relevant items maintained in working memory. J. Neurosci. *32*, 12411–12420.
12. Merlet, I., Birot, G., Salvador, R., Molaee-Ardekani, B., Mekonnen, A., Soria-Frish, A., Ruffini, G., Miranda, P.C., and Wendling, F. (2013). From oscillatory transcranial current stimulation to scalp EEG changes: a biophysical and physiological modeling study. PLoS ONE *8*, e57330.
13. Reato, D., Rahman, A., Bikson, M., and Parra, L.C. (2010). Low-intensity electrical stimulation affects network dynamics by modulating population rate and spike timing. J. Neurosci. *30*, 15067–15079.
14. Ali, M.M., Sellers, K.K., and Fröhlich, F. (2013). Transcranial alternating current stimulation modulates large-scale cortical network activity by network resonance. J. Neurosci. *33*, 11262–11275.
15. Schmidt, S.L., Iyengar, A.K., Foulser, A.A., Boyle, M.R., and Fröhlich, F. (2014). Endogenous cortical oscillations constrain neuromodulation by weak electric fields. Brain Stimul. *7*, 878–889.
16. Vosskuhl, J., Huster, R.J., and Herrmann, C.S. (2015). Increase in short-term memory capacity induced by down-regulating individual theta frequency via transcranial alternating current stimulation. Front. Hum. Neurosci. *9*, 257.
17. Polanía, R., Nitsche, M.A., Korman, C., Batsikadze, G., and Paulus, W. (2012). The importance of timing in segregated theta phase-coupling for cognitive performance. Curr. Biol. *22*, 1314–1318.
18. Fuentemilla, L., Penny, W.D., Cashdollar, N., Bunzeck, N., and Düzel, E. (2010). Theta-coupled periodic replay in working memory. Curr. Biol. *20*, 606–612.
19. Rutishauser, U., Ross, I.B., Mamelak, A.N., and Schuman, E.M. (2010). Human memory strength is predicted by theta-frequency phase-locking of single neurons. Nature *464*, 903–907.
20. Macmillan, N., and Creelman, D. (2005). Detection Theory: A User's Guide, Second Edition (Psychology Press).
21. Fell, J., and Axmacher, N. (2011). The role of phase synchronization in memory processes. Nat. Rev. Neurosci. *12*, 105–118.
22. Kaplan, R., Bush, D., Bonnefond, M., Bandettini, P.A., Barnes, G.R., Doeller, C.F., and Burgess, N. (2014). Medial prefrontal theta phase coupling during spatial memory retrieval. Hippocampus *24*, 656–665.
23. Polanía, R., Paulus, W., and Nitsche, M.A. (2012). Noninvasively decoding the contents of visual working memory in the human prefrontal cortex within high-gamma oscillatory patterns. J. Cogn. Neurosci. *24*, 304–314.
24. Foster, B.L., Dastjerdi, M., and Parvizi, J. (2012). Neural populations in human posteromedial cortex display opposing responses during memory and numerical processing. Proc. Natl. Acad. Sci. USA *109*, 15514–15519.
25. Logothetis, N.K., Eschenko, O., Murayama, Y., Augath, M., Steudel, T., Evrard, H.C., Besserve, M., and Oeltermann, A. (2012). Hippocampal-cortical interaction during periods of subcortical silence. Nature *491*, 547–553.
26. Voytek, B., Kayser, A.S., Badre, D., Fegen, D., Chang, E.F., Crone, N.E., Parvizi, J., Knight, R.T., and D'Esposito, M. (2015). Oscillatory dynamics coordinating human frontal networks in support of goal maintenance. Nat. Neurosci. *18*, 1318–1324.
27. Barbey, A.K., Koenigs, M., and Grafman, J. (2013). Dorsolateral prefrontal contributions to human working memory. Cortex *49*, 1195–1205.
28. Buzsáki, G., and Moser, E.I. (2013). Memory, navigation and theta rhythm in the hippocampal-entorhinal system. Nat. Neurosci. *16*, 130–138.
29. McNab, F., and Klingberg, T. (2008). Prefrontal cortex and basal ganglia control access to working memory. Nat. Neurosci. *11*, 103–107.
30. Roux, F., and Uhlhaas, P.J. (2014). Working memory and neural oscillations: alpha-gamma versus theta-gamma codes for distinct WM information? Trends Cogn. Sci. *18*, 16–25.
31. Clayton, M.S., Yeung, N., and Cohen Kadosh, R. (2015). The roles of cortical oscillations in sustained attention. Trends Cogn. Sci. *19*, 188–195.
32. Fujisawa, S., and Buzsáki, G. (2011). A 4 Hz oscillation adaptively synchronizes prefrontal, VTA, and hippocampal activities. Neuron *72*, 153–165.
33. Watrous, A.J., Deuker, L., Fell, J., and Axmacher, N. (2015). Phase-amplitude coupling supports phase coding in human ECoG. eLife *4*, e07886.
34. Buzsáki, G., Anastassiou, C.A., and Koch, C. (2012). The origin of extracellular fields and currents—EEG, ECoG, LFP and spikes. Nat. Rev. Neurosci. *13*, 407–420.
35. Qiu, C., Shivacharan, R.S., Zhang, M., and Durand, D.M. (2015). Can neural activity propagate by endogenous electrical field? J. Neurosci. *35*, 15800–15811.
36. Fröhlich, F., and McCormick, D.A. (2010). Endogenous electric fields may guide neocortical network activity. Neuron *67*, 129–143.
37. Ozen, S., Sirota, A., Belluscio, M.A., Anastassiou, C.A., Stark, E., Koch, C., and Buzsáki, G. (2010). Transcranial electric stimulation entrains cortical neuronal populations in rats. J. Neurosci. *30*, 11476–11485.
38. Allen, E.A., Liu, J., Kiehl, K.A., Gelernter, J., Pearlson, G.D., Perrone-Bizzozero, N.I., and Calhoun, V.D. (2011). Components of cross-frequency modulation in health and disease. Front. Syst. Neurosci. *5*, 59.
39. de Hemptinne, C., Ryapolova-Webb, E.S., Air, E.L., Garcia, P.A., Miller, K.J., Ojemann, J.G., Ostrem, J.L., Galifianakis, N.B., and Starr, P.A. (2013). Exaggerated phase-amplitude coupling in the primary motor cortex in Parkinson disease. Proc. Natl. Acad. Sci. USA *110*, 4780–4785.

40. Peirce, J.W. (2009). Generating stimuli for neuroscience using PsychoPy. Front. Neuroinform. *2*, 10.

41. Ambrus, G.G., Al-Moyed, H., Chaieb, L., Sarp, L., Antal, A., and Paulus, W. (2012). The fade-in—short stimulation—fade out approach to sham tDCS—reliable at 1 mA for naïve and experienced subjects, but not investigators. Brain Stimul. *5*, 499–504.

42. Antal, A., and Paulus, W. (2013). Transcranial alternating current stimulation (tACS). Front. Hum. Neurosci. *7*, 317.

43. Thielscher, A., Antunes, A., and Saturnino, G.B. (2015). Field modeling for transcranial magnetic stimulation: a useful tool to understand the physiological effects of TMS? 37th Annual International Conference of the IEEE Engineering in Medicine and Biology Society (EMBC), 222–225.

44. Opitz, A., Paulus, W., Will, S., Antunes, A., and Thielscher, A. (2015). Determinants of the electric field during transcranial direct current stimulation. Neuroimage *109*, 140–150.

45. Geuzaine, C., and Remacle, J.-F. (2009). Gmsh: a 3-D finite element mesh generator with built-in pre- and post-processing facilities. Int. J. Numer. Methods Eng. *79*, 1309–1331.

46. Hentschke, H., and Stüttgen, M.C. (2011). Computation of measures of effect size for neuroscience data sets. Eur. J. Neurosci. *34*, 1887–1894.

47. Oostenveld, R., Fries, P., Maris, E., and Schoffelen, J.-M. (2011). FieldTrip: open source software for advanced analysis of MEG, EEG, and invasive electrophysiological data. Comput. Intell. Neurosci. *2011*, 156869.

48. Vinck, M., Oostenveld, R., van Wingerden, M., Battaglia, F., and Pennartz, C.M.A. (2011). An improved index of phase-synchronization for electrophysiological data in the presence of volume-conduction, noise and sample-size bias. Neuroimage *55*, 1548–1565.

49. Xia, M., Wang, J., and He, Y. (2013). BrainNet Viewer: a network visualization tool for human brain connectomics. PLoS ONE *8*, e68910.